

Synthesis and Reactivity in Inorganic, Metal-Organic, and Nano-Metal Chemistry

Publication details, including instructions for authors and subscription information:

<http://www.tandfonline.com/loi/lsrt20>

Synthesis, Characterization, and Cytotoxic Activity on MCF-7 Cell Line of Some Novel Metal Complexes With Substituted Benzimidazole Ligands

Ahmed M. A. El-Seidy ^{a b}, Eman El-Zahany ^a, Atiat S. Barakat ^c, Nabil S. Youssef ^a, Shadia A. Galal ^d & Sayed A. Drweesh ^a

^a Inorganic Chemistry Department, National Research Center, Cairo, Egypt

^b Department of Chemistry, Faculty of Science, The Imam Muhammad bin Saud Islamic University, Riyadh, Saudi Arabia

^c Inorganic Chemistry Department, Faculty of Science, Zagazig University, El Zagazig, Egypt

^d Department of Chemistry of Natural and Microbial Products, Division of Pharmaceutical and Drug Industries Research, National Research Centre, Cairo, Egypt

Accepted author version posted online: 06 Aug 2012. Version of record first published: 03 Dec 2012.

To cite this article: Ahmed M. A. El-Seidy, Eman El-Zahany, Atiat S. Barakat, Nabil S. Youssef, Shadia A. Galal & Sayed A. Drweesh (2013): Synthesis, Characterization, and Cytotoxic Activity on MCF-7 Cell Line of Some Novel Metal Complexes With Substituted Benzimidazole Ligands, *Synthesis and Reactivity in Inorganic, Metal-Organic, and Nano-Metal Chemistry*, 43:1, 46-56

To link to this article: <http://dx.doi.org/10.1080/15533174.2012.682691>

PLEASE SCROLL DOWN FOR ARTICLE

Full terms and conditions of use: <http://www.tandfonline.com/page/terms-and-conditions>

This article may be used for research, teaching, and private study purposes. Any substantial or systematic reproduction, redistribution, reselling, loan, sub-licensing, systematic supply, or distribution in any form to anyone is expressly forbidden.

The publisher does not give any warranty express or implied or make any representation that the contents will be complete or accurate or up to date. The accuracy of any instructions, formulae, and drug doses should be independently verified with primary sources. The publisher shall not be liable for any loss, actions, claims, proceedings, demand, or costs or damages whatsoever or howsoever caused arising directly or indirectly in connection with or arising out of the use of this material.

Synthesis, Characterization, and Cytotoxic Activity on MCF-7 Cell Line of Some Novel Metal Complexes With Substituted Benzimidazole Ligands

Ahmed M. A. El-Seidy,^{1,2} Eman El-Zahany,¹ Atiat S. Barakat,³ Nabil S. Youssef,¹ Shadia A. Galal,⁴ and Sayed A. Drweesh¹

¹Inorganic Chemistry Department, National Research Center, Cairo, Egypt

²Department of Chemistry, Faculty of Science, The Imam Muhammad bin Saud Islamic University, Riyadh, Saudi Arabia

³Inorganic Chemistry Department, Faculty of Science, Zagazig University, El Zagazig, Egypt

⁴Department of Chemistry of Natural and Microbial Products, Division of Pharmaceutical and Drug Industries Research, National Research Centre, Cairo, Egypt

A series of novel metal complexes with the Schiff base ligands 4-(((1H-benzo[d]imidazol-2-yl)methyl)imino)methyl)benzene-1,3-diol, H_3L^1 , and (((1H-benzo[d]imidazol-2-yl)methyl)thio)propanenitrile, HL^2 , have been synthesized and identified by elemental and spectral (UV-vis, IR, ¹H NMR, mass) analyses, molar conductivities, as well as magnetic moment measurements technique. The ligands behave either as neutral tridentate or bidentate ligand. The antitumor activity of the new compounds was tested against breast cancer cell line MCF-7. Ag and Cu complexes 2, 8 and 9 showed a remarkable smaller value of IC₅₀ than that of the Tamoxifen, the standard. This would provide a new potential antitumor drug that deserves more attention.

Keywords benzimidazole complexes, cytotoxic activity, human breast cancer cell line (MCF-7), Schiff base metal complexes

1. INTRODUCTION

The benzimidazole ring is an important pharmacophore in modern drug discovery.^[1] Benzimidazole derivatives exhibit significant activity against several viruses such as HIV, herpes (HSV-1), RNA, influenza, and human cytomegalovirus (HCMV).^[2] Benzimidazole and its derivatives have been used to act as topoisomerase inhibitors, selective neuropeptide Y Y1 receptor antagonists, angiotensin II inhibitors, inhibitors of HCMV replication, 5-HT₃ antagonists in isolated guinea pig ileum, potential antitumor agents, antimicrobial agents, smooth muscle cell proliferation inhibitors, a treatment for interstitial cystitis, and in diverse areas of chemistry.^[3] In addition, benzim-

idazoles are very important intermediates in organic reactions.^[4] Cancer is thought to reflect a multistep process, resulting from an accumulation of inherited and/or acquired defects in genes involved in the positive or negative regulation of cell proliferation and survival.^[5] Breast cancer has been defined as an abnormal division or proliferation of epithelial cell in lactiferous duct or lobe and can be classified into ductal carcinoma and lobular carcinoma.^[6] The importance of metal compounds in medicine dates back to the 16th century with reports on the therapeutic use of metals or metal-containing compounds in the treatment of cancer. Now the list of therapeutically prescribed metal-containing compounds includes platinum (anticancer), silver (antimicrobial), gold (antiarthritic), bismuth (antiulcer), antimony (antiprotozoal), vanadium (antidiabetic), and iron (antimalarial).^[7] Metal ions are electron deficient, whereas most biological molecules (proteins and DNA) are electron rich; consequently, there is a general tendency for metal ions to bind to and interact with many important biological molecules. Metal ions also have a high affinity for many small molecules (e.g., O₂) that are crucial to life. These considerations alone have fueled much of the past and current interest in developing novel means to use metals or metal containing agents to modulate biological systems.^[8] Schiff bases of azomethine nitrogen donor heterocyclic ligands are well known due to their wide range of applications in pharmaceutical and industrial fields.^[9] Transition metal complexes of Schiff bases have attracted a lot of interest due to their potent biological activities such as antifungal, antibacterial, anticancer, and herbicidal applications.^[9,10] These studies have shown that complexation of metals to Schiff base ligands improves the antimicrobial and anticancer activities of the ligands.^[9,11] A group of complex compounds of 2-aminobenzimidazole derivatives with some metals, such as cobalt, zinc, and copper, showed also antifungal and antibacterial activity.^[12] While complexes with ruthenium were cytotoxic

Received 15 March 2012; accepted 31 March 2012.

Address correspondence to Ahmed M. A. El-Seidy, Inorganic Chemistry Department, National Research Centre, P.O. 12622, Dokki, Giza, Egypt. E-mail: ahmedmaee2@gmail.com.

in vitro against SKW-8 cells (human T-lymphoma).^[13] The main target of present work is to study the coordination behavior of the benzimidazole ligands H_3L^1 and HL^2 that incorporate many binding sites towards Ag^I , Cu^{II} , Fe^{III} , Pt^{II} , Ru^{III} , Ni^{II} , and Zn^{II} ions. The structures of the ligands and their metal complexes were elucidated by elemental analysis, IR, 1H NMR, ^{13}C NMR, UV-vis, mass spectra, conductivity, and magnetic susceptibility measurements at room temperature. The biological activity of the present organic ligands and their metal complexes are also reported. The remarkable smaller value of IC₅₀ of Ag and Cu complexes **2**, **8** and **9**, than that of the Tamoxifen would provide a new potential antitumor drug that deserves more attention.

EXPERIMENTAL

Materials and Methods

All the reagents and solvents employed for the preparation of the ligand and its complexes were of the best grade available and used without further purification. 2-aminomethylbenzimidazoldihydrochloride and 2,4-dihydroxybenzaldehyde were prepared according to the literature procedures.^[14,15]

Physical Measurements

The ligands and their metal complexes were analyzed for C, H, N, and S contents at the Microanalytical Laboratory, Faculty of Science, Cairo University, Egypt, but all other analyses were carried out at Microanalytical Laboratories, National Research Centre, Dokki, Giza, Egypt. Analytical and physical data of the ligands H_3L^1 and HL^2 and their metal complexes are reported in (Table 1). The metal ion contents of the complexes were also determined by the previously reported methods.^[16–19] IR spectra of the ligands and their metal complexes were measured using KBr discs with a Jasco FT/IR 300E Fourier transform infrared spectrophotometer covering the range 400–4000 cm^{-1} and in the 500–100 cm^{-1} region using polyethylene-sandwiched Nujol mulls on a Perkin-Elmer FT-IR 1650 spectrophotometer. 1H

NMR spectra were obtained on Bruker Avance 300-DRX or Avance 400-DRX spectrometers. Chemical shifts (ppm) are reported relative to TMS. The electronic spectra of the ligands and their complexes were obtained in Nujol mulls using a Shimadzu UV-240 UV-visible recording spectrophotometer. Molar conductivities of the metal complexes in DMSO (10^{-3} M) were measured using a dip cell and a Bibby Scientific Limited conductimeter MC1 at room temperature. The resistance measured in ohms and the molar conductivities were calculated according to the equation: $\Lambda = V \times K \times Mw/g \times \Omega$, where Λ is molar conductivity ($ohm^{-1} cm^2 mol^{-1}$), V is the volume of the complex solution (mL), K is the cell constant $0.92 cm^{-1}$, Mw the molecular weight of the complex, g is weight of the complex, and Ω is resistance measured in ohms. Magnetic moments at 298 K were determined using the Gouy method with $Hg[Co(SCN)_4]$ as calibrant. Mass spectra of the solid ligand were recorded using JEUL JMS-AX-500 mass spectrometer.

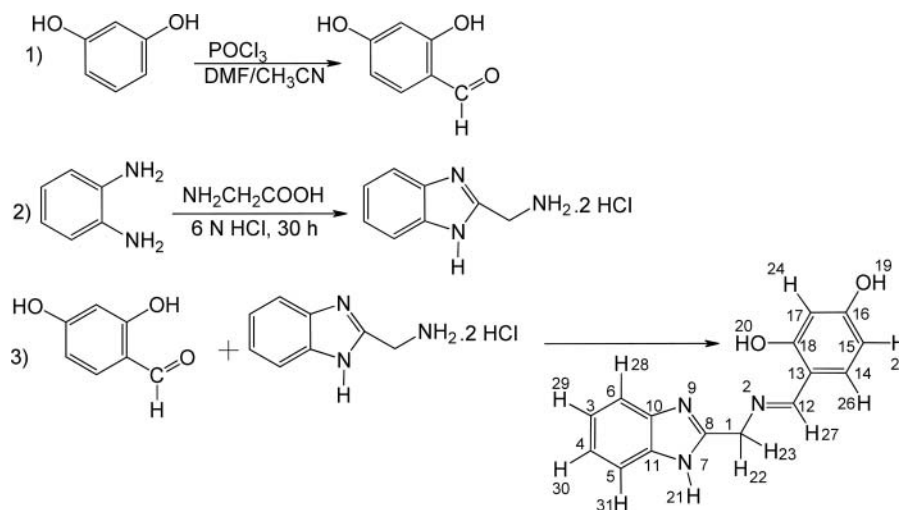
Synthesis of the Schiff Base Ligands

Synthesis of 4-(((1H-benzo[d]imidazol-2-yl)methyl)imino)methyl)benzene-1,3-diol, H_3L^1

The methanol solution (40 mL) of 2-aminomethylbenzimidazoldihydrochloride (4.42 g, 20.0 mmol) was neutralized by NaOH, then filtrated to remove the sodium chloride precipitation. The filtrate was then added to the solution of 2,4-Dihydroxybenzaldehyde (2.76 g, 20.0 mmol) in methanol (20 mL). The reaction mixture was stirred for 1 h. The excess solvent was evaporated under reduced pressure. The formed yellow precipitate is washed several times by ethanol and dried under vacuum over anhydrous $CaCl_2$ (Scheme 1).

Synthesis of (((1H-benzo[d]imidazol-2-yl)methyl)thio)propane-nitrile, HL^2

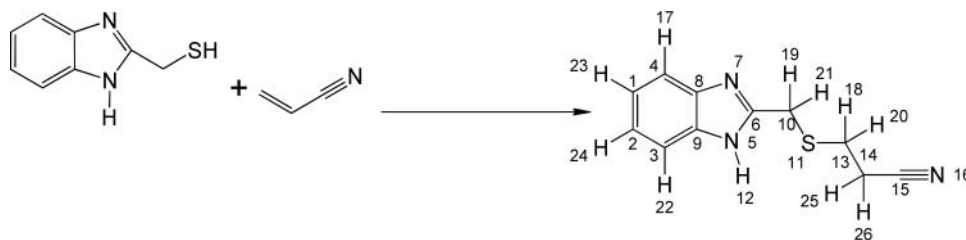
A mixture of 2-thiomethylbenzimidazole (1.64 g, 10 mmol) and potassium hydroxide (0.56 g, 10 mmol) in MeOH (50 mL) was stirred for 15 min then acrylonitrile (0.53 g, 10 mmol) was



SCH. 1. Schematic representation for the formation of the Schiff base ligand H_3L^1 and its numbering.

TABLE 1
Analytical and physical data of the ligands H_3L^1 and HL^2 and their metal complexes

No.	Ligands/Complexes	Color	FW	Yield (%)	Found(Anal. Calcd.) (%)					Molar conductance $\Delta m(\Omega^{-1} \text{ cm}^2 \text{ mol}^{-1})$
					C	H	N	S	M	
1	H_3L^1 $C_{15}H_{13}N_3O_2$	yellow	267.3	72	67.3(67.4)	4.8(4.9)	15.8(15.7)	—	—	—
2	$H_3L^1 AgONO_2$ $C_{15}H_{13}AgN_4O_5$	yellow	437.2	79	41.3(41.2)	3.1(3.0)	12.7(12.8)	—	24.8(24.7)	21
3	$H_3L^1 Cu(OC(O)CH_3)_2$ $C_{19}H_{19}CuN_3O_6$	brown	448.9	86	50.7(50.8)	4.2(4.3)	9.3(9.4)	—	14.3(14.2)	18
4	$H_3L^1 FeCl_3$ $C_{15}H_{13}Cl_3FeN_3O_2$	brown	429.5	82	42.1(42.0)	3.2(3.1)	9.7(9.8)	—	13.1(13.0)	24
5	$[H_3L^1 PtCl]Cl$ $C_{15}H_{13}Cl_2N_3O_2Pt$	yellow	533.3	79	33.7(33.8)	2.6(2.5)	8.0(7.9)	—	36.5(36.6)	84
6	$H_3L^1 RuCl_3$ $C_{15}H_{12}Cl_3N_3O_2Ru$	brown	473.7	72	37.9(38.0)	2.8(2.6)	9.0(8.9)	—	21.1(21.3)	23
7	HL^2 $C_{11}H_{11}N_3S$	yellow	217.3	70	60.8(60.8)	5.1(5.1)	19.3(19.3)	14.7(14.8)	—	—
8	$HL^2 Ag(ONO_2)(H_2O)$ $C_{11}H_{13}AgN_4O_4S$	yellow	405.2	69	32.5(32.6)	3.3(3.2)	13.9(13.8)	7.7(7.9)	26.7(26.6)	18
9	$HL^2 Cu(OC(O)CH_3)_2(H_2O)_2$ $C_{15}H_{21}CuN_3O_6S$	brown	435.0	88	41.5(41.4)	4.9(4.9)	9.8(9.7)	7.5(7.4)	14.7(14.6)	22
10	$(HL^2)_2 Ni(OC(O)CH_3)_2$ $C_{26}H_{28}NiO_4S_2$	reddish brown	611.4	84	51.2(51.1)	4.7(4.6)	13.7(13.8)	10.6(10.5)	9.5(9.6)	23
11	$HL^2 PtCl_2$ $C_{11}H_{11}Cl_2N_3PtS$	yellow	483.3	76	27.4(27.3)	2.3(2.3)	8.7(8.7)	6.5(6.6)	40.2(40.1)	28
12	$HL^2 ZnCl_2$ $C_{11}H_{11}Cl_2N_3SZn$	yellow	353.6	68	37.5(37.4)	3.2(3.1)	11.8(11.9)	9.0(9.1)	18.6(18.5)	22



SCH. 2. Schematic representation for the formation of the Schiff base ligand **HL**² and its numbering.

added. The reaction mixture was stirred for 2 h. The excess solvent was evaporated under reduced pressure. The salt was collected and dissolved in cold water then, acidified by drops of hydrochloric acid. The solid formed was filtered off and washed with cold water then, crystallized from methanol as orange powder (Scheme 2).

Synthesis of the Metal Complexes

The following general procedure was used in the synthesis of all metal complexes. The salts—AgNO₃ (0.84 g, 5 mmol), Cu(CH₃COO)₂ (0.90 g, 5 mmol), FeCl₃·6H₂O (1.35 g, 5 mmol), Ni(CH₃COO)₂·4H₂O (1.24 g, 5 mmol), ZnCl₂ (0.68 g, 5 mmol) and RuCl₃·3H₂O (1.30 g, 5 mmol)—were dissolved in a hot (70°C) methanol solution (25 mL) and the solution was added to a hot (70°C), stirred ethanolic solution (25 mL) of the corresponding ligand H₃L¹ (1.33 g, 5 mmol) and HL² (1.08 g, 5 mmol for all complexes except Ni [2.17 g, 10 mmol] was used). The mixture was left under reflux with continuous stirring for 5 h and the solid complexes precipitated. The resulting solid was filtered off, washed several times with methanol and then with diethyl ether, and dried under vacuum at 50°C for 5 h. In case of platinum(II) compounds a stock [PtCl₄]²⁻ solution was used by dissolving PtCl₂ (2.66 g, 10 mmol) in concentration HCl (until dissolved) under reflux, and the turbidity of the undissolved material is then removed by filtration. The solution is then neutralized with Na₂CO₃ and diluting with distilled water up to 250 mL (pH 6.0–6.5) to yield a solution of 0.04 M [PtCl₄]²⁻, then (125 mL, 5 mmol) was used.^[20]

Biological Evaluation

The cytotoxic activity was measured *in vitro* for the newly synthesized compounds using the sulfoRhodamine-B stain (SRB) assay using the method of Skehan at The National Cancer Institute, Cairo University, Cairo, Egypt.^[21]

Test compounds were dissolved in DMSO and diluted with saline to the appropriate volumes. Different concentrations of the compound under test (5.0, 12.5, 25.50, and 50.0 μg/mL) were added to the cell monolayer. Tamoxifen, a standard and well-known anticancer drug, was used as a standard drug to evaluate the relative cytotoxic efficiency of the tested compounds at the same concentrations.

The relation between surviving fraction and drug concentration is plotted to get the survival curve. The results of cytotoxic activity were expressed as an IC₅₀; the dose of compound (in

μg/mL), that inhibits proliferation rate of the tumor cells by 50% as compared with control untreated cells.

RESULTS AND DISCUSSION

Elemental Analysis

The elemental and physical data of the ligands and their complexes (Table 1) showed that the stoichiometry of the complexes obtained is either 1:1 or 1:2 M/L (metal:ligand).

Mass Spectra of the Ligands

The mass spectra of the Schiff bases H₃L¹ and HL² revealed the molecular ion peaks at *m/e* 267 and 217, which is coincident with the formulae weights 267.3 and 217.3, respectively, for these compounds and supports the identity of their structures.

Conductivity Measurements

All metal complexes are stable in air and insoluble in common organic solvents but soluble in DMSO. The molar conductivities of the complexes in DMSO (10⁻³ M) are listed in Table 1. Only complex **5** behaved as a 1:1 electrolyte. The elevated value of the conductance of this complex may be due to partial dissociation of the coordinated chlorine with the solvent molecules.^[22] The rest of the complexes showed a non-electrolyte nature.^[23]

Infrared Spectra

The infrared spectra of the ligands showed sharp band in the 3375–3405 cm⁻¹ region due to NH_{benzimidazole}, which remain unchanged after complexation indicating that it was not involved in complex formation. The band due to ν(OH) stretching vibration of ligand H₃L¹ was found as strong band around 3230 cm⁻¹,^[24] while the sharp band located around 1620 cm⁻¹ was assigned to ν(C=N) stretch. The presence of hydrogen bonding between NH of benzimidazole and other electronegative atoms in ligand is indicated by the appearance of several medium intensity bands in the range 2500–2700 cm⁻¹. These bands are also present in complexes indicating the presence of hydrogen bonding in complexes.^[25] The IR data of the Schiff bases H₃L¹ and HL² and their complexes are listed in (Table 2). The IR spectra of the complexes are compared with those of the free ligand in order to determine the coordination sites that may be involved in chelation. In all complexes of H₃L¹, the ligand behaved as neutral tridentates ligand coordinating through both

TABLE 2
IR frequencies of the bands (cm^{-1}) of ligands H_3L^1 and HL^2 and their metal complexes and their assignments.

No.	Ligands/Complexes	$\nu(\text{H}_2\text{O})$	$\nu(\text{OH})$	$\nu(\text{NH})$	$\nu(\text{C}=\text{N})$ and ν ($\text{C}=\text{N}$) _{Benz}	$\nu(\text{C}-\text{O})$	$\nu(\text{C}\equiv\text{N})$	$\nu(\text{C}-\text{S})$	$\nu_s(\text{Coo}), \nu_{as}(\text{Coo}^-),$ (Δ), $\nu(\text{NO}_3)$
1	H_3L^1	—	3230br	3375br	1621br	1220s	—	—	—
2	$\text{H}_3\text{L}^1\text{AgONO}_2$	—	3232br, 3189br	3381br	1617v.s, 1600s	1226vs	—	—	1448, 1360, 1075, 699
3	$\text{H}_3\text{L}^1\text{Cu}(\text{OC}(\text{O})\text{CH}_3)_2$	—	3234br, 3197br	3377br	1604v.s	1230s	—	—	1580, 1366, 214
4	$\text{H}_3\text{L}^1\text{FeCl}_3$	—	3230br, 3185br	3379br	1603v.s	1230s	—	—	—
5	$[\text{H}_3\text{L}^1\text{PtCl}]\text{Cl}$	—	3231br, 3194br	3378br	1623v.s, 1607sh	1227s	—	—	—
6	$[\text{H}_3\text{L}^1\text{RuCl}_2(\text{H}_2\text{O})]\text{Cl}$	3441br	3234br, 3189br	3378br	1612v.s, 1599sh	1230	—	—	—
7	HL^2	—	—	3400br	1618s	—	2251w	700w, 645w	—
8	$\text{HL}^2\text{Ag}(\text{ONO}_2)(\text{H}_2\text{O})$	3464br	—	3405br	1600w	—	2249w	655m, 610m	1452, 1364, 1055, 710
9	$\text{HL}^2\text{Cu}(\text{OC}(\text{O})\text{CH}_3)_2(\text{H}_2\text{O})_2$	3450br	—	3404br	1606m	—	2249w	670m, 615w	1570, 1362, 208
10	$(\text{HL}^2)_2\text{Ni}(\text{OC}(\text{O})\text{CH}_3)_2$	—	—	3404br	1595s	—	2250w	650m, 630w	1563, 1340, 223
11	HL^2PtCl_2	—	—	3402br	1603s	—	2248w	650w, 618w	—
12	HL^2ZnCl_2	—	—	3406br	1605sh	—	2248w	654s, 630m	—

imine groups and one hydroxyl group (NNO). These complexes showed a shift to lower wave number with decreasing intensity of the bands of both imine's and one of the hydroxyl groups indicating they are involved in coordination to the central metal while the other hydroxyl group almost retained its original positions indicating it was not involved in coordination.^[26,27] The appearance of two bands due to $\nu(\text{C-O})$ one almost at its original position while the other was shift to higher wave number further supports the coordination of only one of the two phenolic oxygen to the central metal.^[27] In case of the ligand H_3L^2 complexes, the ligand behaved as neutral bidentate ligand coordinating through the imine and thio-ether groups. The IR data of these complexes showed a shift to lower wave number in the band corresponding to the imine group along with a decrease in its intensity, indicating its involvement in coordination.^[26-30] The thio-ether band in the free ligand appeared as a split band at 700 and 645 cm^{-1} . However, this mode is shifted in the spectra of the complexes and appeared at 670–650 cm^{-1} and 630–610 cm^{-1} suggesting the bonding of the metal ion through sulfur atom of the ligand.^[31] The most important absorption occurred at 2251 cm^{-1} and corresponds to the $\nu_{\text{as}}(\text{C}\equiv\text{N})$ stretching, which remain unchanged in complexes excluding participation of this group in complexation.^[32] The new bands in spectra of all complexes in the 435–475, 334–380, and 520–570 cm^{-1} regions were assigned to $\nu(\text{M-N})$, $\nu(\text{M-S})$, and $\nu(\text{M-O})$ vibrations, respectively.^[33,34] The acetato group in complexes **3**, **9**, and **10** acted as a monodentate ligand and this is supported by the appearance of two new bands in the ranges 1580–1560 cm^{-1} and 1366–1340 cm^{-1} , which may be attributed to $\nu_{\text{asym.}}(\text{COO}^-)$ and $\nu_{\text{sym.}}(\text{COO}^-)$, respectively.^[35] The separation value (Δ) between $\nu_{\text{asym.}}(\text{COO}^-)$ and $\nu_{\text{sym.}}(\text{COO}^-)$ in these complexes were more than 200 cm^{-1} (208–223 cm^{-1}), suggesting the coordination of carboxylate group in a monodentate fashion.^[36] Further, the complex exhibits $\delta(\text{COO}^-)$ at 750 cm^{-1} , which is considered diagnostic for monodentate acetates.^[35] The broad bands in 3464–3441 cm^{-1} region in the spectra of complexes **6**, **8**, and **9** are due to coordinated water rather than water of crystallization. This is supported by the presence of bands at 1585–1595, 925–950, and 600–625 cm^{-1} due to H_2O deformation, H_2O rocking, and H_2O wagging, respectively.^[37,38] The spectrum of nitrate complexes **2** and **8** showed bands in 1452–1448 (ν_1), 1075–1055 (ν_2), 1364–1360 (ν_4), and 710–699 (ν_5) regions

TABLE 3

The electronic absorption spectral bands (nm) and magnetic moment (B.M.) for the ligands H_3L^1 HL^2 and their metal complexes

No.	Ligands/ Complexes	λ_{max} (nm) (ϵ [$\text{mol}^{-1} \text{cm}^{-1}$])	μ_{eff} in BM
1	H_3L^1	312, 381, 462	—
2	$\text{H}_3\text{L}^1\text{AgONO}_2$	290, 325, 395, 465, 550	—
3	$\text{H}_3\text{L}^1\text{Cu}(\text{OC}(\text{O})\text{CH}_3)_2$	285, 330, 415, 455, 650	1.74
4	$\text{H}_3\text{L}^1\text{FeCl}_3$	290, 320, 430, 465, 750	5.9
5	$[\text{H}_3\text{L}^1\text{PtCl}]\text{Cl}$	300, 340, 410, 460	—
6	$[\text{H}_3\text{L}^1\text{RuCl}_2(\text{H}_2\text{O})]\text{Cl}$	295, 325, 410, 460, 590, 675	1.85
7	HL^2	300, 340, 402	—
8	$\text{HL}^2\text{Ag}(\text{ONO}_2)(\text{H}_2\text{O})$	310, 330, 365, 420, 468, 560	—
9	$\text{HL}^2\text{Cu}(\text{OC}(\text{O})\text{CH}_3)_2(\text{H}_2\text{O})_2$	315, 370, 430, 745	1.89
10	$(\text{HL}^2)_2\text{Ni}(\text{OC}(\text{O})\text{CH}_3)_2$	315, 350, 410, 585, 815	3.45
11	HL^2PtCl_2	295, 320, 354, 425	—
12	HL^2ZnCl_2	290, 325, 360, 440	—

with ν_1 – ν_4 separation of 88 cm^{-1} , characteristic of monodentate nitrate group.^[39]

Electronic Spectra and Magnetic Moments

The structure of the ligand reveals that the two lone pairs of electrons of azo group are not the only interacting non-bonding electrons because the ligand contains nitrogen and oxygen atoms, which also may be extra sources of lone pair of electrons. Thus, other $n \rightarrow \pi^*$ transition is expected to take place from these non-bonding orbital to different π^* molecular

TABLE 4
(a): $^1\text{H-NMR}$ spectral data of H_3L^1 and some of its metal complexes

Compound	H(21)	H(19), H(20)	H(27)	H(28), H(31)H(24), H(26)	H(29), H(30)	H(25)	H(22), H(23)
H_3L^1	13.61br	13.05(s, 1H), 12.67(s, 1H)	8.62(s, 1H)	7.55(m, 4H)	7.25(dd, 2H)	6.41(s, 1H)	4.97(s, 2H)
2	13.60br	13.04(s, 1H), 12.60(s, 1H)	8.47(s, 1H)	7.59(m, 4H)	7.25(dd, 2H)	6.40(s, 1H)	5.03(s, 2H)
6	13.61s	13.05(s, 1H), 12.53(s, 1H)	8.39(s, 1H)	7.59(m, 4H)	7.15(dd, 2H)	6.47 (s, 1H)	4.93(s, 2H)

TABLE 5
¹H-NMR spectral data of HL²

Compound	H(12)	H(17), H(22)	H(23), H(24)	H(19), H(21)	H(18), H(20), H(25), H(26)
HL ²	13.40 (br, 1H)	7.54 (S, 2H)	7.17 (S, 2H)	4.04(s, 2H)	2.86(m, 4H)

orbital extending over such a large molecule. The data (Table 3) reveal that the ligand comprises three sets of bands in the UV and visible regions.^[40] The first set of the shortest wavelength is 300–340 nm range, which may be assigned to the $\pi \rightarrow \pi^*$ transition in the aromatic moiety and intraligand $\pi \rightarrow \pi^*$ transition.^[41] The second set appears in the 381–402 nm range, which may be assigned to $n \rightarrow \pi^*$ of the azomethine group.^[42] The band located in the visible region at 462 nm can be assigned to $\pi \rightarrow \pi^*$ transition involving the whole electronic system of the compounds with a considerable charge transfer character arising mainly from the phenolic moiety.^[40,43] The spectral data of the free ligands and their metal complexes in DMSO are listed in Table 3. The spectra of the diamagnetic Ag(I) complexes (**2**, **8**) exhibited two bands in the 550–560, 465–468, and 365–395 nm ranges; the latter two may arise from charge transfer of the type may arise from charge transfer of the type ligand (π) \rightarrow b_{1g} (Ag⁺) and ligand (σ) \rightarrow b_{1g} (Ag⁺), respectively, in a typically distorted square planar environment around the metal ion.^[44–46] The electronic spectra of the copper complex **3** showed a band

at 650 nm and ascribed to the d-d transition (dxz; dyz \rightarrow dx²-y²). These results are typical of square pyramidal geometry,^[47] while complex **9** exhibited a band at 745 nm range assignable to ²E_g \rightarrow ²T_g transition, which is the expected band for d⁹ ion in an octahedral configuration with low crystal field splitting.^[48] The magnetic moments of the copper complexes at room temperature lied in 1.74–1.89 B.M. range (Table 3), corresponding to one unpaired electron.^[49] The electronic spectrum of the ferric complex **4** showed a band at 750 nm, that may be assigned to ⁶A₁ \rightarrow ⁴T₁(G), indicating distorted octahedral geometry around Fe(III) ion.^[50,51] The magnetic moment of this complex was found to be 5.9 B.M. and fall within the range observed for octahedral Fe(III) complexes.^[52–54] The ruthenium complex **6** showed two bands at 675 and 590 nm. The ground state of ruthenium(III) in octahedral environment is ²T_{2g}, arising from the t⁵_{2g} configuration, and the first excited doublet levels in the order of increasing energy are ²A_{2g} and ²T_{1g}, arising from the t⁴_{2g}e¹_g configuration. Hence, these two bands may correspond to ²T_{2g} \rightarrow ²A_{2g} and ²T_{2g} \rightarrow ²T_{1g}. Thus, the pattern of the

TABLE 6
Thermal data for the metal complexes

No.	Temp. (°C)	DTA (Peak)	TGA (wt. loss%), Anal. Calcd. (Found)	Assignment	Composition of the residue
3	265	Endo	26.31(26.55)	Loss of 2 acetate groups	[H ₃ L ¹ Cu]
	325	Endo	–	Melting point	[H ₃ L ¹ Cu]
	560	Exo	17.72(18.09)	Decomposition and formation of CuO	CuO
4	250	Endo	24.76(25.04)	Loss of three chloride ions	[H ₃ L ¹ Fe]
	315	Endo	–	Melting point	[H ₃ L ¹ Fe]
	550	Exo	37.18(37.58)	Decomposition and formation of Fe ₂ O ₃	Fe ₂ O ₃
6	268	Endo	22.41(22.74)	Loss of three chloride ions	[H ₃ L ¹ Ru]
	290	Endo	–	Melting point	[H ₃ L ¹ Ru]
	645	Exo	52.69(52.98)	Decomposition and formation of Ru ₂ O ₃	Ru ₂ O ₃
9	137	Endo	8.28(8.54)	Loss of two coordinated water	[HL ² Cu(OC(O)CH ₃) ₂]
	260	Endo	27.15(27.42)	Loss of two acetate groups	[HL ² Cu]
	340	Endo	–	Melting point	[HL ² Cu]
10	510	Exo	18.29(18.38)	Decomposition and formation of CuO	CuO
	245	Endo	19.32(19.58)	Loss of 2 acetate groups	[(HL ²) ₂ Ni]
	275	Endo	–	Melting point	[(HL ²) ₂ Ni]
12	615	Exo	12.22(12.44)	Decomposition and formation of NiO	NiO
	270	Endo	20.05(20.35)	Loss of two chloride ions	[HL ² Zn]
	310	Endo	–	Melting point	[HL ² Zn]
	520	Exo	23.02(23.37)	Decomposition and formation of ZnO	ZnO

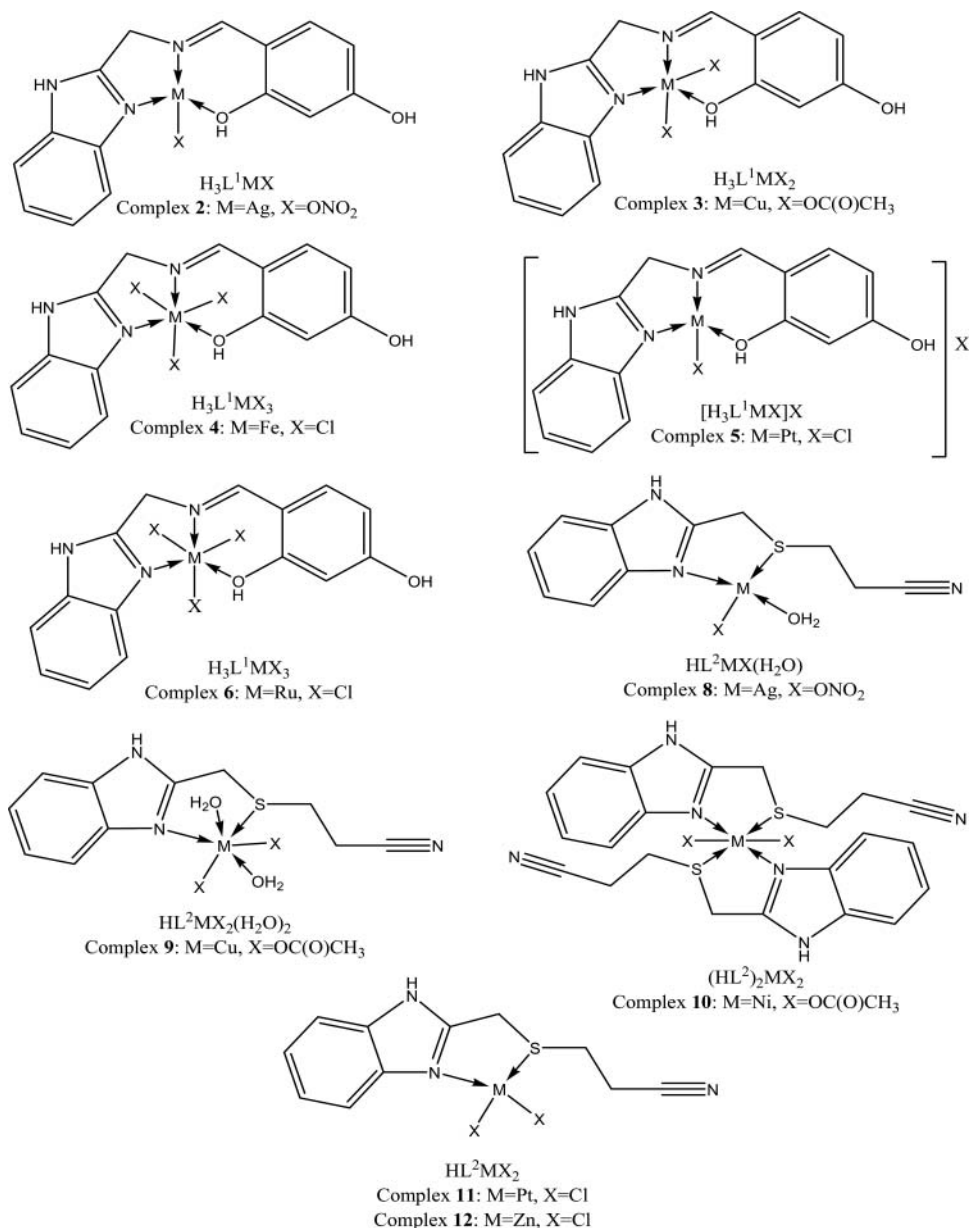


FIG. 1. The proposed structures of metal complexes.

electronic spectra of the ruthenium (III) complex indicates the presence of an octahedral environment around the ruthenium (III) ion.^[24,53,55–57]

The electronic spectrum of Nickel(II) complex, complex 10, showed bands at 815 and 585 nm that may be arising from $^3A_2g \rightarrow ^3T_1g(F)$ and $^3A_2g \rightarrow ^3T_1g(P)$ transitions, respectively in octahedral geometry.^[58–60]

¹HNMR Studies of the Ligands and Some of Their Diamagnetic Complexes

The insolubility of the complexes in the other organic solvents necessitates recording ¹H NMR spectra in dimethylsulfoxide-*d*₆ (DMSO-*d*₆) (Tables 4 and 5).

The ¹HNMR spectrum of the ligand H_3L^1 showed three signals at 13.61, 13.05, and 12.67 ppm. The former was assigned to $NH_{imidazole}$ while the other signals were assigned the phenolic OH's protons. These signals disappeared on the addition of D₂O. The singlet at 8.62 ppm was assigned to $CH=N$ proton. The signals in the 7.55–6.41 ppm range may be due to the aromatic rings protons. The signal due to the $-CH_2-$ appeared as a singlet at 4.97. The singlet of the $NH_{imidazole}$ showed no significant shift in the spectrum of all complexes, indicating it is not involved in complexation. The signals at 12.67 showed downfield shift in the spectra of complexes 2 and 6 while the other signal at 13.05 almost retained its original position. This supports that only on phenolic oxygen is involved in complex

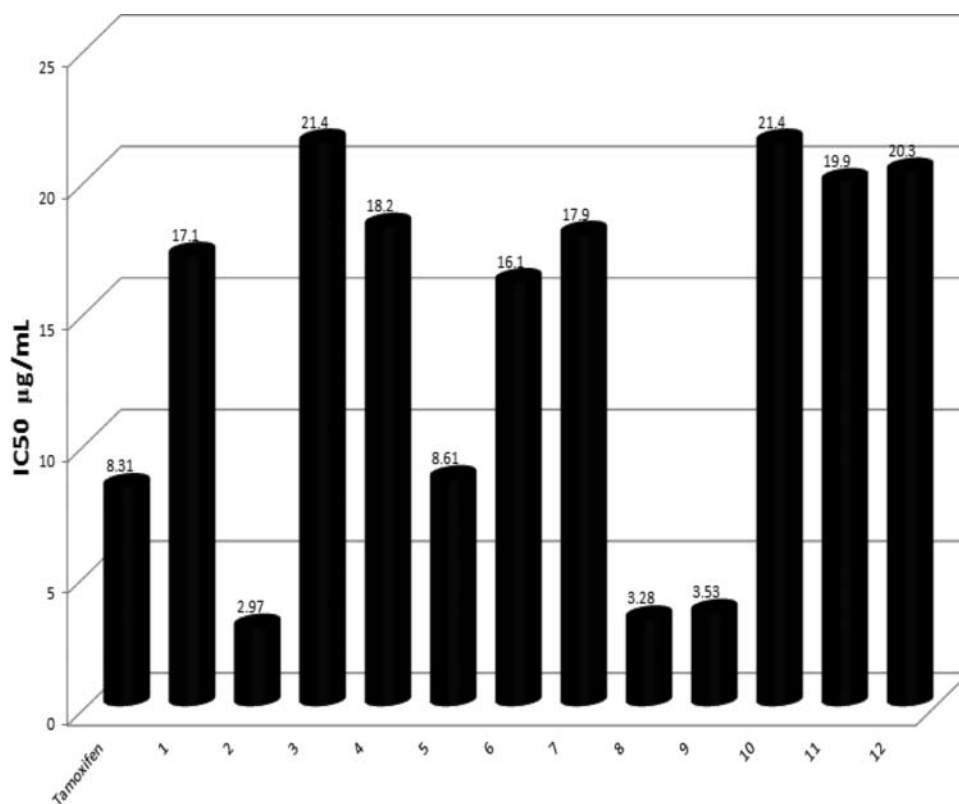


FIG. 2. Cytotoxic activities of ligands and their complexes against human breast cancer cell line (MCF-7).

formation. The singlet at 8.62 ppm showed a downfield shift ($\Delta\delta = 0.15\text{--}0.23$ ppm) on complex formation, which indicates the coordination of the azomethine nitrogen to the central metal. The ^1H NMR spectrum of the ligand HL^2 showed a signal at 13.40 assigned to $\text{NH}_{\text{imidazole}}$. The signals in the 7.54–7.17 ppm range may be due to the aromatic rings protons. The signals due to the $-\text{CH}_2-$ appeared in 4.04–2.86 ppm range.

Thermal analyses (DTA and TGA)

The results of DTA and TGA of complexes **3**, **4**, **6**, **9**, **10**, and **12** are shown in Table 6. The results showed good agreement with the theoretical formulae as suggested from the analytical data.

Biological Activities

This study has shown that the two ligands and their metal complexes were cytotoxic against human breast cancer cell line (MCF-7). The cytotoxic activity of the Schiff base ligands H_3L^1 and HL^2 could be attributed to the antiproliferative activity of hydroxyl group and the occurrence of $\text{C}\equiv\text{N}$ moiety, respectively, which may be an important fragment for hydrogen bonding formation at the receptor site.^[61–63] Also, the study has shown that complexation of metals to the Schiff base ligands improves the anticancer activities of the ligands (**2**, **5**, **6**, **8**, and **9**). This may be attributed to the lipophilic character of the central metal atom explained by Tweedy's chelation theory.^[11,64] The decreased

activity of complexes (**3**, **4**) and (**10–12**) compared to that of ligands (**1**, **7**) could be attributed to their poor solubility than their respective free ligands.^[65] Additionally, the current comparative study with Tamoxifen, and based on the IC₅₀ values

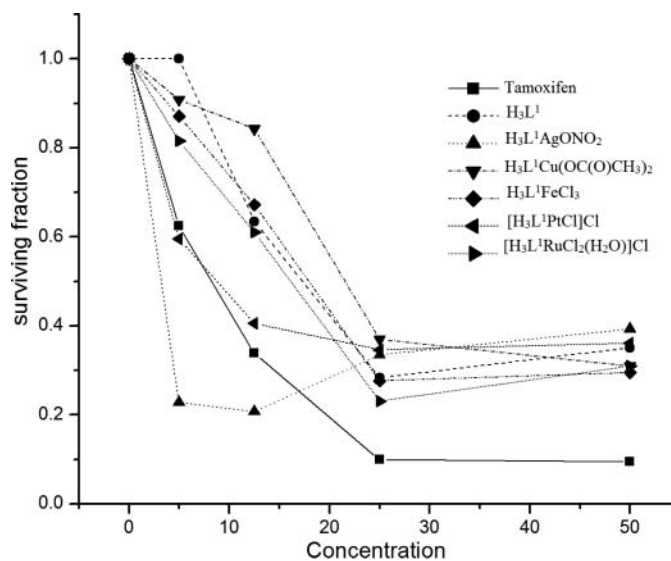


FIG. 3. Effect of different concentrations of ligand H_3L^1 and its complexes on the viability of human breast cancer cell line (MCF-7).

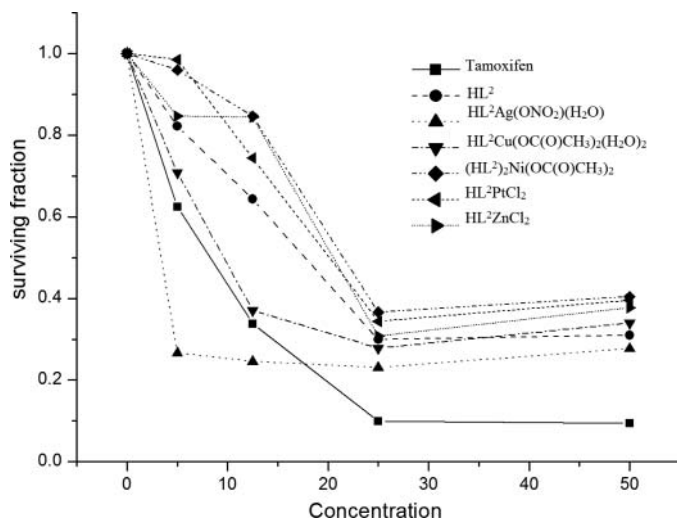


FIG. 4. Effect of different concentrations of ligand HL^2 and its complexes on the viability of human breast cancer cell line (MCF-7).

obtained with human breast cancer cell line (MCF-7) revealed that the H_3L^1 ligand and HL^2 -silver complexes were between 2.53 and 2.8 and HL^2 -copper complexes were 3.35 times more cytotoxic than Tamoxifen, whereas the Ag(I) complexes induce apoptosis (programmed cell death) in cancer cells which may be a direct result of their action on the cell, while copper complexes would cause intracellular generation of hydroxyl radicals from H_2O_2 produced during normal cellular activities by the reduction of Cu(II) to Cu(I), leading to a growth inhibition in tumor cells.^[66] The ligand HL^2 and its complexes, except complexes **8** and **9**, showed a very low reactivity and we can regard the reactivity in case of complexes **8** and **9** to the presence of copper and silver ions. The very high reactivity in case of complex **9** compared to the low reactivity of complex **3** is due to the presence of sulfur in the ligand HL^2 . Since sulfur is a medium-soft base it stabilizes copper in the low oxidation state and hence facilitates the reduction of Cu(II) to Cu(I). This reduction will increase the formation of hydroxyl radicals from H_2O_2 . Oxygen is a hard base and stabilizes the presences of copper in the high oxidation state. The close cytotoxic value of H_3L^1 -platinum complex **11** to Tamoxifen value supports the use of cisplatin and related platinum complexes as anti-cancer agents, which has stimulated a search for other active transition metal complexes, which are as or more effective but with fewer side effects.^[63]

The IC₅₀ values were summarized as shown in Figure 2 and the effect of different concentrations of the ligands and their complexes on the viability of human breast cancer cell line (MCF-7) are shown in Figures 3 and 4.

CONCLUSION

In the present work, we synthesized two novel Schiff base ligands H_3L^1 and HL^2 and their Ag^I, Cu^{II}, Fe^{III}, Pt^{II}, Ru^{III}, Ni^{II}, and Zn^{II}. The ligands and their metal complexes have been synthesized and identified by elemental analyses, molar conductivities,

and spectral (UV-Vis, IR, ¹H NMR, ¹³C NMR, mass) and magnetic moment measurements techniques. The ligands behaved either as neutral tridentate or neutral bidentate ligands. Conductance measurements suggest the non-electrolytic nature for all the metal complexes except complex **5**, which behaves as a 1:1 electrolyte. Complexes **2**, **8**, and **9** showed a remarkable smaller value of IC₅₀ than that of Tamoxifen, which would provide a new potential antitumor drug that deserves more attention.

REFERENCES

1. Tebbe, M.J.; Spitzer, W.A.; Victor, F.; Miller, S.C.; Lee, C.C.; Sattelberg, T.R.; McKinney, E.; Tang, C.J. *J. Med. Chem.* **1997**, *40*, 3937–3946.
2. Tamm, I. *Science* **1957**, *126*, 1235–1236.
3. Iyenger, S.; Nuhhauser, M.A.; Thor, K.B. U.S. Patent 1, **1996**.
4. Bai, Y.; Lu, J.; Shi, Z.; Yang, B. *Synth. Lett.* **2001**, 544.
5. El-Deeb, I. M.; Lee, S. H. *Bioorgan. Med. Chem.* **2010**, *18*, 3860–3874.
6. Lin, Y.-L.; Su, Y.-T.; Chen, B.-H. *Eur. J. Pharmacol.* **2010**, *637*, 1–10.
7. Desoize, B. *Crit. Rev. Oncol. Hematol.* **2002**, *42*, 213–215.
8. Huang, R.; Wallqvist, A.; Covell, D.G. *Biochem. Pharmacol.* **2005**, *69*, 1009–1039.
9. Karthikeyan, M.S.; Prasad, D.J. *Bioorg. Med. Chem.* **2006**, *14*, 7482–7489.
10. Singh, K.; Barwa, M.S.; Tyagi, P. *Eur. J. Med. Chem.* **2007**, *42*, 394–402.
11. Creaven, B.S.; Duff, B.; Egan, D.A.; Kavanagh, K.; Rosair, G.; Thangella, V.R.; Walsh, M. *Inorg. Chim. Acta* **2010**, *363*, 4048–4058.
12. Kukalenko, S.S.; Udovenko, V.A.; Borysova, V.P.; Kulugina, N.L.; Burmakina, N.M.; Andreeva, E.L.; U.S.S.R. SU 1,636,414. *Odkrytiya Izobret* **1991**, *11*, 75–165.
13. Nikolova, D.; Ivanov, R.; Buyukliev, S.; Konstantinov, M.; Karaivanova, M.; Arzheim-Forsch, A. *Drug Res.* **2001**, *51*, 758–762.
14. Mendelson, W.L.; Hayden, S. *Synth. Commun.* **1996**, *26*, 603–610.
15. Cescon, L.A.; Day, A.R. *J. Org. Chem.* **1962**, *27*, 581.
16. Welcher, F.J. *The Analytical Uses of Ethylenediamine Tetraacetic Acid*. Van Nostrand: New York, **1958**.
17. Vogel, A.I. *Textbook of Practical Organic Chemistry, Including Qualitative Organic Analysis*. Longman: London, **1978**.
18. Holzbecher, Z.; Divis, L.; Kral, M.; Sucha, L.; Vracil, F. *Handbook of Organic Reagents in Inorganic Analysis*. Wiley: Chichester, England, **1976**.
19. El-Sonbati, A.Z.; El-Bindary, A.A.; Al-Sarawy, A.A. *Spectrochim. Acta, Part A* **2002**, *58*, 2771–2778.
20. Kovala-Demertzi, D.; Yadav, P.N.; Demertzis, M.A.; Coluccia, M. J. *Inorg. Biochem.* **2000**, *78*, 347–354.
21. Skehan, P.; Storeng, R.; Scudiero, D.; Monks, A.; Mahon, J.; Vistica, D.; Warren, J.T.; Bokesch, H.; Kenney, S.; Boyd, M.R. *J. Nat. Cancer Ins.* **1990**, *82*, 1107–1112.
22. El-Bindary, A.A. *Trans. Met. Chem.* **1997**, *22*, 381–384.
23. Golcu, A.; Tumer, M.; Demirelli, H.; Wheatley, R.A. *Inorg. Chim. Acta* **2005**, *358*, 1785–1797.
24. Kannan, S.; Ramesh, R. *Polyhedron* **2006**, *25*, 3095.
25. Maurya, M.R.; Chandrakar, A.K.; Chand, S. *J. Mol. Catal. A: Chem.* **2007**, *263*, 227–237.
26. Youssef, N. S.; El-Zahany, E.; El-Seidy, A.M.A.; Caselli, A.; Fantauzzi, S.; Cenini, S. *Inorg. Chim. Acta* **2009**, *362*, 2006–2014.
27. Nakatamoto, K. *Infrared Spectra of Inorganic and Coordination Compounds*. Wiley Interscience: New York, **1970**.
28. El-Wahab, Z.H.A.; Mashaly, M.M.; Salman, A.A.; El-Shetary, B.A.; Faheim, A.A. *Spectrochim. Acta Part A* **2004**, *60*, 2861–2873.
29. Youssef, N. S.; El-Zahany, E. A.; El-Seidy, A. M. A.; Caselli, A.; Cenini, S. *J. Mol. Catal. A: Chem.* **2009**, *308*, 159–168.
30. El-Tabl, A.S.; El-Saied, F.A.; Al-Hakimi, A.N. *Transition Met. Chem.* **2007**, *32*, 689–701.
31. Sarkar, S.; Dey, K. *Spectrochim. Acta, Part A* **2005**, *62*, 383–393.

32. Yuste, C.; Armentano, D.; Marino, N.; Canadillas-Delgado, L.; Delgado, F.S.; Ruiz-Perez, C.; Rillema, D.P.; Lloret, F.; Julve, M. *Dalton Trans.* **2008**, 1583–1596.
33. Singh, K.; Barwa, M.S.; Tyagi, P. *Eur. J. Med. Chem.* **2006**, *41*, 147–153.
34. Patel, R. N.; Gundla, V.L.N.; Patel, D.K. *Polyhedron* **2008**, *27*, 1054–1060.
35. Nakamoto, K. *Infrared and Raman Spectra of Inorganic and Coordination Compounds*. Wiley: New York, **1986**.
36. Boghaei, D.M.; Gharagozlou, M. *Spectrochim. Acta A* **2007**, *67*, 944–949.
37. El-Dissouky, A.; Fahmy, A.; Amer, A. *Inorg. Chim. Acta* **1987**, *133*, 311–316.
38. Teotia, M.P.; Gurtu, J.N.; Rana, V.B. *J. Inorg. Nucl. Chem.* **1980**, *42*, 821–831.
39. Sonza, P.; Garcia-Vfizquez, A.J.; Masaguer, J.R. *Transition Met. Chem.* **1985**, *10*, 410–412.
40. Rageh, N. M.; Mawgoud, A.M.A.; Mostafa, H.M. *Chem. Papers* **1999**, *53*, 107–113.
41. Raj, B.N.B.; Kurup, M.R.P.; Suresh, E. *Spectrochim. Acta, Part A* **2008**, *71*, 1253–1260.
42. Gup, B.K.R. *Spectrochim. Acta, Part A* **2005**, *62*, 1188–1195.
43. R. Gup. Giziroglu, E.; Kirkan, B. *Dyes Pigments* **2007**, *73*, 40–46.
44. Sabin, F.; Ryu, C.K.; Fork, P.; Vogler, A. *Inorg. Chem.* **1992**, *31*, 1941–1946.
45. Mostafa, S.I.; Bekheit, M.M. *Chem. Pharm. Bull. Jpn.* **2000**, *48*, 266–271.
46. Mostafa, S.I.; Ikeda, S.; Ohtani, B. *J. Mol. Catal. A: Chem.* **2005**, *225*, 181–188.
47. Matsumoto, K.; Sekine, N.; Arimura, K.; Ohba, M.; Ohba, H.; Sakiyama, H.; Okawa, H. *Bull. Chem. Soc. Jpn.* **2004**, *77*, 1343–1351.
48. Sanmartin, J.; Novio, F.; Garcia-Deibe, A.M.; Fondo, M.; Ocampo, N.; Bermejo, M.R. *Polyhedron* **2006**, *25*, 1714–1722.
49. Mohamed, G.G.; El-Gamel, N.E.A. *Spectrochim. Acta, Part A* **2004**, *60*, 3141–3154.
50. Sallam, S.A.; Orabi, A.S.; El-Shetary, B.A.; Lentz, A. *Transition Met. Chem.* **2002**, *27*, 447–453.
51. Singh, N.K.; Singh, S.B. *Transition Met. Chem.* **2001**, *26*, 487–495.
52. Garcia-Friaza, G.; Fernandez-Botello, A.; Perez, J. M.; Prieto, M. J.; Moreno, V. J. *Inorg. Biochem.* **2006**, *100*, 1368–1377.
53. El-Tabl, A.S.; El-Saied, F.A.; Al-Hakimi, A.N. *Transition Met. Chem.* **2007**, *32*, 689.
54. Singh, N.K. *Transition Met. Chem.* **2001**, *26*, 487–495.
55. Balasubramanian, K.P.; Parameswari, K.; Chinnusamy, V.; Prabhakaran, R.; Natarajan, K. *Spectrochim. Acta Part A* **2006**, *65*, 678–683.
56. Nehru, K.; Athappan, P.; Rajagopal, G. *Transition Met. Chem.* **2001**, *26*, 652–656.
57. El-Tabl, A.S.; Issa, R.M.; Morsi, M.A. *Transition Met. Chem.* **2004**, *29*, 543–549.
58. Ali, M.A.; Mirza, A.H.; Bujang, F.H.; Hamid, M.H.S.A.; Bernhardt, P.V. *Polyhedron* **2006**, *25*, 3245–3252.
59. Krishnapriya, K.R.; Kandaswamy, M. *Polyhedron* **2005**, *24*, 113–120.
60. Gudasi, K.B.; Patil, M.S.; Vadavi, R.S.; Shenoy, R.V.; Patil, S.A.; Nethaji, M. *Transition Met. Chem.* **2006**, *31*, 580–584.
61. El-Azab, A.S.; Al-Omar, M.A.; Abdel-Aziz, A.A.M.; Abdel-Aziz, N.I.; El-Sayed, M.A.A.; Aleisa, A.M.; Sayed-Ahmed, M.M.; Abdel-Hamide, S.G. *Eur. J. Med. Chem.* **2010**, *45*, 4188–4198.
62. Moreau, E.; Fortin, S.; Lacroix, J.; Patenaude, A.; Rousseau, J.; Gaudreault, R.-C. *Bioorg. Med. Chem.* **2008**, *16*, 1206–1217.
63. Thati, B.; Noble, A.; Creaven, M.W.B.S.; McCann, M.; Kavanagh, K.; Devereux, M.; Egan, D.A. *Cancer Lett.* **2007**, *248*, 321–331.
64. Youssef, N.S.; El-Zahany, E.A.; Ali, M.M. *Phosphorus, Sulfur Silicon Relat. Elem.* **2010**, *185*, 2171–2181.
65. Gottschaldt, M.; Peiffer, A.; Koth, D.; Gorls, H.; H.-Dahse, M.; Mollmann, U.; Obata, M.; Yano, S. *Tetrahedron* **2006**, *62*, 11073–11080.
66. Byrnes, R. W.A.; W. E. Petering, D.H. *Free Rad. Biol. Med.* **1992**, *13*, 469–478.